

4.09 LONG RANGE LIGHTNING NOWCASTING APPLICATIONS FOR METEOROLOGY

Nicholas W.S. Demetriades, Martin J. Murphy and Ronald L. Holle
Vaisala, Inc., Tucson, Arizona

1. INTRODUCTION

Real-time lightning detection data are used for a variety of meteorological and aviation applications over land areas where cloud-to-ground lightning (CG) networks cover all or part of 40 countries. Real-time CG data are typically combined with radar and other information to identify significant weather over a wide range of time and space scales.

The outer limit of land-based CG flash detection networks is set at 625 km from sensors in the U.S. National Lightning Detection Network (NLDN) and the Canadian Lightning Detection Network (CLDN). This distance is determined by characteristics of the radiation emitted by the ground waves from CG flashes (Section 2). While 625 km is beyond the range of coastal meteorological radars, it is not especially far from land for convective weather systems that often translate and evolve at velocities of 50 km per hour or more.

The primary sources of information about thunderstorms over the oceans beyond the 625-km range are satellite imagery, as well as pilot and ship reports. Satellite scans are often collected at 30-minute intervals with a subsequent time delay in availability. Ship reports are sparse, and sporadic pilot reports are often delayed in time. As a result, flights over oceans can enter convective regions with little or no warning. Aircraft can encounter turbulence, icing, direct lightning strikes, and other hazards that can be avoided over and near land regions where there are CG lightning and radar networks (Nierow et al., 2002). Similarly, shipping and other offshore interests have a relatively small amount of information on convective activity beyond the range of the nearest land-based radar.

Vaisala is conducting an ongoing experiment to operate a VLF long-range lightning detection network (LLDN) over the Atlantic and Pacific Oceans to detect flashes thousands of kilometers from sensors in North America, Europe and Asia. The following study describes results in two regions, the extratropical areas and the tropics. In extratropical regions, frequent lightning has been found in cyclones during the cold season over the oceans. The detection of lightning in such cyclones has shown that flashes are often an indicator of future storm development, intensification, and precipitation intensity. In the tropics, outbreaks of lightning within eyewalls of some hurricanes near the coast had been studied with respect to eyewall contraction or secondary eyewall replacement. The prior research has been expanded to strong hurricanes over much larger areas than previously possible. In

addition, detection of flashes in outer rainbands of tropical cyclones may provide forecasters with a valuable diagnostic tool. For many areas that do not experience the inner core of the hurricane, intense outer rainbands contain the most hazardous weather. In weaker tropical cyclones, such as tropical depressions and storms, intense rainbands often contain the highest wind speeds and heaviest rainfall.

2. LONG-RANGE LIGHTNING DETECTION NETWORK (LLDN)

NLDN and CLDN wideband sensors operate in the frequency range from about 0.5 and 400 kHz where return strokes in CG flashes radiate most strongly. The peak radiation from CG flashes comes near 10 kHz in the middle of the very low frequency (VLF) band of 3-30 kHz. Signals in the VLF band are trapped in the earth-ionosphere waveguide and suffer relatively less severe attenuation than higher frequency signals. Low frequency (LF) and VLF ground wave signals from CGs are attenuated strongly, and are almost imperceptible after a propagation distance of 500 to 1000 km. However VLF signals may be detected several thousand kilometers away after one or more reflections off the ground and the ionosphere. Detection is best when both a lightning source and a sensor are on the night side of the earth, because of better ionospheric propagation conditions at night. The NLDN can easily detect and process signals from lightning at long distances because the standard sensors in the networks detect across a broad band that includes all of the VLF.

Standard NLDN sensors have been part of an ongoing experimental long-range detection network consisting of the combination of the CLDN, the Japanese Lightning Detection Network, the Meteo-France network, and the BLIDS, Benelux, and Central European networks operated by Siemens in Germany. This combination of networks detects CG flashes in sufficient numbers and with sufficient accuracy to identify small thunderstorm areas. The network detects CGs to varying degrees over the northern Atlantic and Pacific oceans, and also over some areas of Asia and Latin America not covered by local ground-based lightning detection networks.

3. OCEANIC EXTRATROPICAL CYCLONE LIGHTNING NOWCASTING APPLICATIONS

Section 3 will review some of the effects that oceanic convection and latent heat release have on extratropical cyclogenesis, and discuss how lightning data can identify these areas. Other applications are the ability of lightning information to help identify short-

*Corresponding author address: Nicholas W.S. Demetriades, Vaisala, Inc., Tucson, AZ 85706; e-mail: nick.demetriades@vaisala.com.

wave troughs, the rapid intensification of oceanic extratropical cyclones, and deep tropical moisture transported along a cold front into the cold sector of a storm. The potential for long-range lightning data to improve numerical simulations of extratropical cyclones is also an advantage of the LLDN. Lightning data, GOES infrared satellite images and surface maps will be used to show examples of these applications. An extended description of these and other cases is in Demetriades and Holle (2005a).

The nature of LLDN data is shown by two examples off the U.S. west and east coasts in December 2002. Figure 1 shows a cyclone approaching the west coast during flow with a westerly component. While the NLDN shows some flashes (red) when the storm comes close to land, the LLDN (blue) detects many more flashes much further offshore. Figure 2 shows the rate to exceed 1600 flashes per hour with the long-range data.

Along the east coast, Figs. 3 and 4 indicate how the NLDN depicted a fairly large portion of the flash extent during a cyclone that developed into a nor'easter. However, the long period of flashes and very high rates exceeding 12,000 flashes per hour are much better depicted by the LLDN.

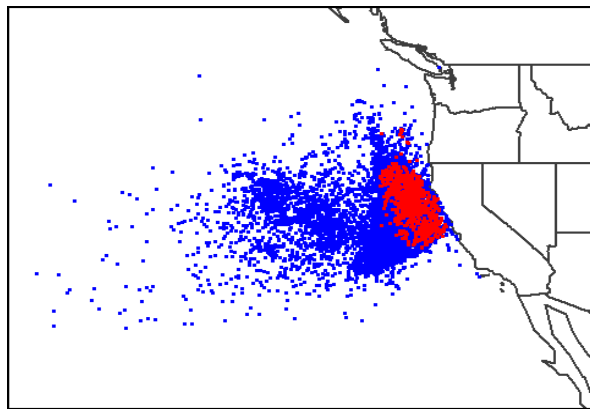


Figure 1. Map of cloud-to-ground (CG) flashes during the approach to the U.S. west coast of a Pacific storm from 17 to 20 December 2002. NLDN flashes are shown in red, and long-range flashes in blue.

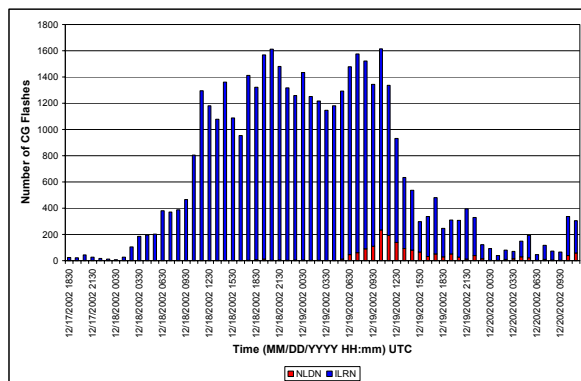


Figure 2. Time series of flashes for Pacific storm in Fig. 1. NLDN flashes in red, and long-range flashes in blue.

From these examples, it can be seen that long-range flashes from the LLDN compared to land-based CGs:

- Cover a larger area,
- Extend the time periods with lightning,
- Detect many more flashes.

3.1 Extratropical Cyclogenesis

Lightning indicates areas of convection where latent heat release into the troposphere is enhanced. In particular, high flash rates over relatively large areas identify regions of large latent heat release that can cause enhanced vertical motion and pressure falls at the surface. Therefore, a widespread area of concentrated lightning activity over the ocean may be one of the first signs of extratropical cyclogenesis.

Lightning can also be generated by the enhanced lift and relatively cold air aloft associated with short wave troughs. As these areas of enhanced upward vertical motion and colder air propagate over relatively warm ocean waters during the winter, they often generate lightning. These short wave troughs can then trigger rapid cyclogenesis as they round the base of a long wave trough. As a result, relatively compact areas

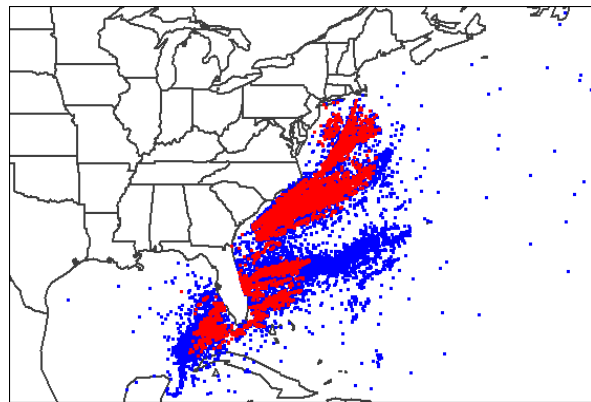


Figure 3. Same as Fig. 1 for Atlantic nor'easter from 24 to 26 December 2002.

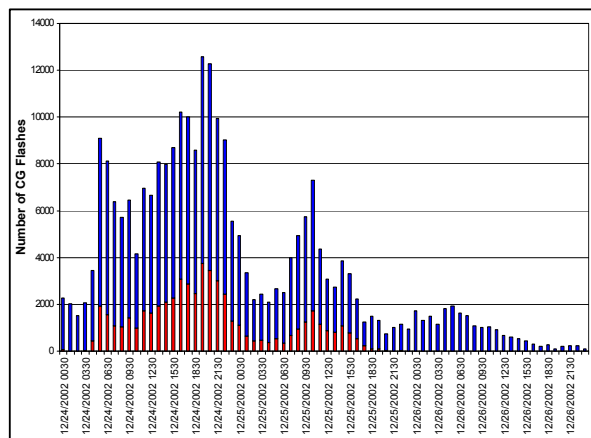


Figure 4. Same as Fig. 2 for storm in Fig. 3.

of lightning activity propagating over the oceans can help identify the existence and intensity of short wave troughs that play a critical role in oceanic cyclogenesis.

Figures 5 to 8 show lightning development over a large area preceding surface extratropical cyclogenesis over the oceans in winter. Figure 5 depicts major pressure centers and fronts at 0000 UTC 7 January 2003. A low is east of the southern New England coast, and a cold front extends through Florida into the Gulf of Mexico. Figure 6 shows substantial lightning developing along the cold front. Lightning continues 6 hours later as a wave of low pressure developed (Fig. 7). By 0900 UTC, a fairly intense extratropical cyclone had developed with a minimum pressure of 996 mb (Fig. 8).

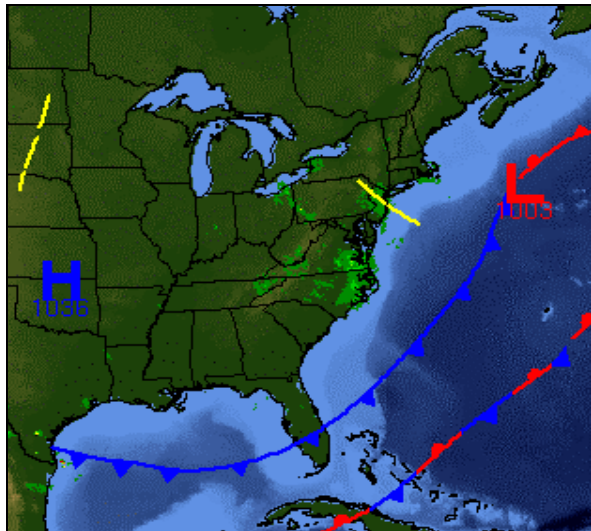


Figure 5. Surface map showing locations of major pressure centers and fronts at 0000 UTC 7 January 2003.

3.2 Extratropical Cyclone Intensity

3.2.1 Lightning near center of an extratropical cyclone

Latent heat release associated with convection can cause rapid intensification of a system if large areas of convection, and by implication lightning, are present near a developing low (Reed and Albright, 1986; Martin and Otkin, 2004). Similarly, large areas of convection along a frontal boundary will cause enhanced frontogenesis due to the increased lift, and by implication convergence, created by latent heating. As a result, the existence of significant lightning rates over open areas of the oceans can help forecasters to identify areas where deep cumulus convection is located and then may influence storm and frontal development.

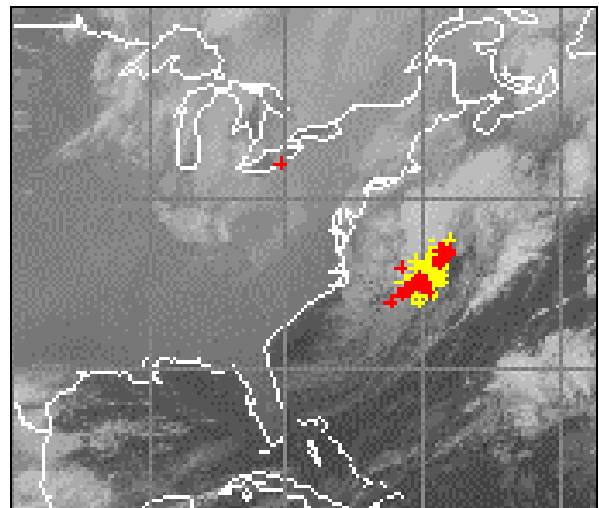


Figure 7. Same as Fig. 6, except for lightning from 0553 to 0853 UTC 7 January 2003. Satellite image is at 0853.

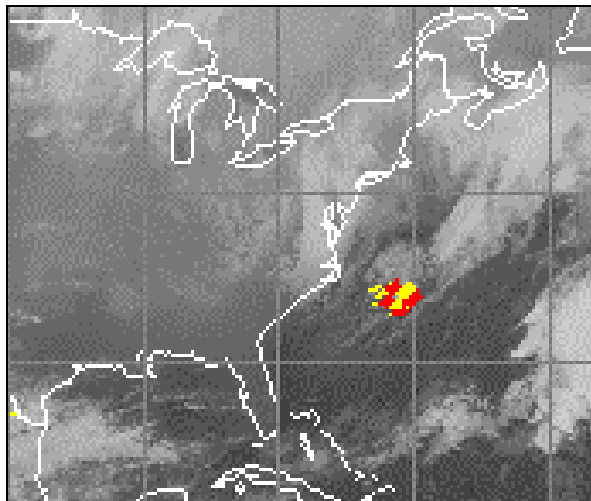


Figure 6. Long range lightning data and infrared satellite image on 6 January 2003. Lightning is for 3 hours from 2053 to 2353 UTC. Yellow dots are flashes detected during the first two hours from 2053 to 2253 UTC, and red are from the latest hour from 2253 to 2353. Satellite image is at 2353.

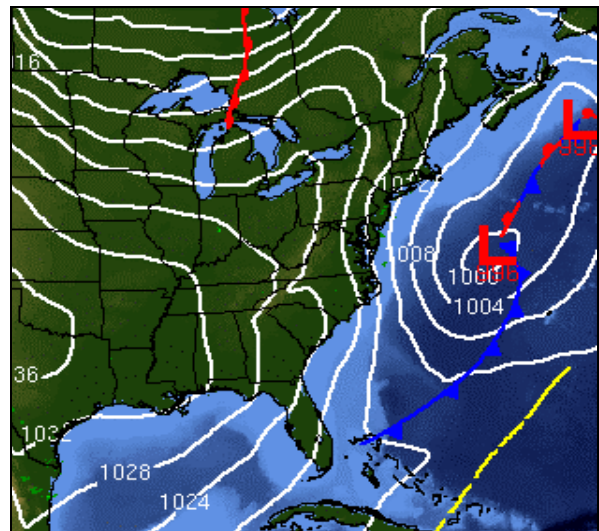


Figure 8. Same as Fig. 5, except for 0900 UTC 7 January.

Lightning development near an existing extratropical cyclone center sometimes may be a response to rapid intensification, rather than a precursor to subsequent intensification. During explosive cyclogenesis, pressure falls cause increased convergence and lift. Lightning may develop if this lift occurs over relatively warm ocean waters with its ample supply of moisture. This sequence is shown by long-range lightning data near the center of an extratropical cyclone southeast of Newfoundland (Figs. 9 and 10). Lightning in Fig. 9 was detected between 1753 and 2053 UTC on 7 January 2003, and the surface map in Fig. 10 is at 2100. The area of active convection is probably not large enough to cause rapid intensification through latent heating. But the initiation of lightning 3

hours earlier near the center of this storm between 1453 and 1753 UTC (not shown), and its persistence through 2053, was coincident with a 13 mb drop in pressure from 992 to 979 mb from 1500 to 2100 UTC 7 January.

3.2.2 Lightning in a short wave trough

Short wave troughs can produce lightning through enhanced lift and colder temperatures aloft. Flashes produced by a short wave trough may be an important complement to satellite imagery to help forecasters identify these important impulses. Such impulses will often round the base of a long-wave trough and cause explosive cyclogenesis as they interact with a pre-existing extratropical cyclone center. Figures 11 and 12 show lightning produced by a short wave trough that is about to interact with a coastal low located off the North Carolina coast. Figure 11 shows the low with a central pressure of 997 mb at 0900 UTC 25 December 2002, and Fig. 12 shows lightning detected between 0600 and 0900 UTC. In this case, the short wave trough and the lightning it was producing were located over North Carolina. This short wave trough caused explosive deepening of the coastal low and by 1800 UTC, its minimum pressure was 979 mb (Fig. 13).

3.2.3 Role of downstream convection on extratropical cyclone intensity and track

Large areas of convection that develop downstream from an extratropical cyclone can greatly influence the storm's intensity, track and precipitation distribution (Alexander et al., 1999; Atallah and Bosart, 2003; Chang et al., 2001). This convection typically develops between the long wave trough and downstream ridge associated with an extratropical cyclone. The convection releases massive amounts of latent heat that raise the heights of mid- and upper-level pressure fields.

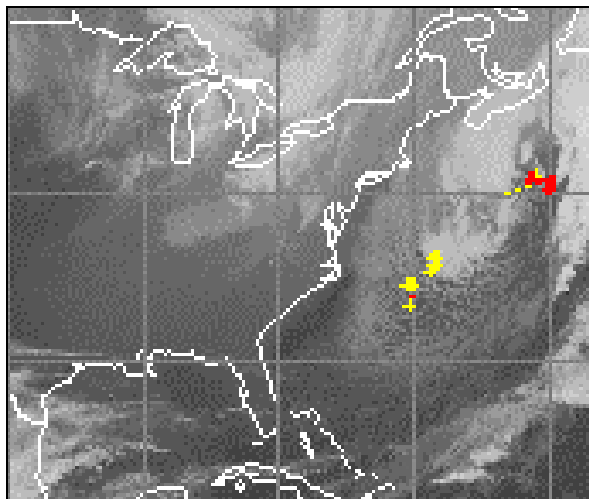


Figure 9. Same as Fig. 6, except for lightning between 1753 and 2053 UTC 7 January 2003. Satellite image is at 2053.

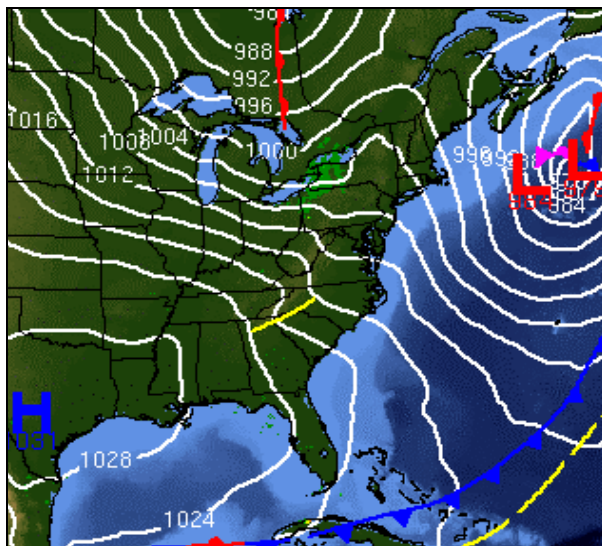


Figure 10. Same as Fig. 5, except at 2100 UTC 7 January.

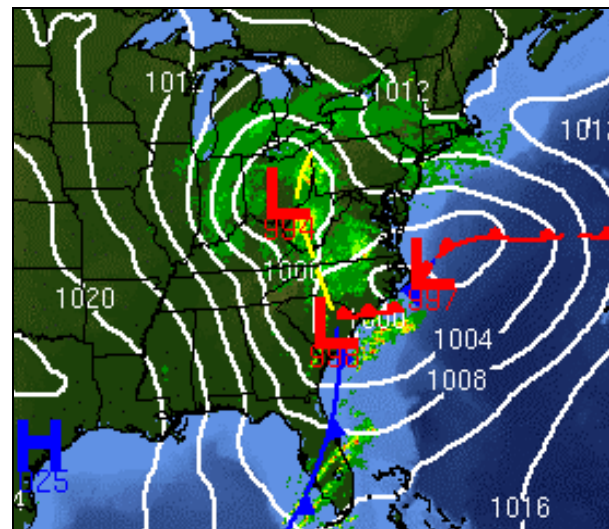


Figure 11. Same as Fig. 5 except for 0900 UTC 25 December 2002. A low is developing just E of North Carolina.

Depending on the location of this convection, it can either amplify the trough and downstream ridge, or cause the trough and downstream ridge to deamplify. The amplification or deamplification of the trough and downstream ridge can cause important changes in extratropical cyclone intensity, track and precipitation distribution. An example in Fig. 14 shows an extremely large area of downstream convection east of the same extratropical cyclone approaching the west coast as was shown by Figs. 1 and 2.

3.2 Cold Front Convection and Winter Precipitation

Very intense lightning activity along the cold front of an extratropical cyclone - but not near the center of the storm - can be an indication of deep tropical moisture

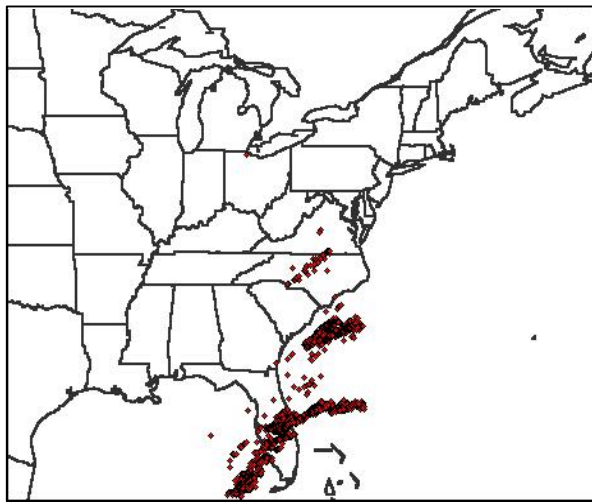


Figure 12. NLDN CG flashes detected between 0600 and 0900 UTC 25 December 2002. The short wave trough over central North Carolina is producing CG lightning.

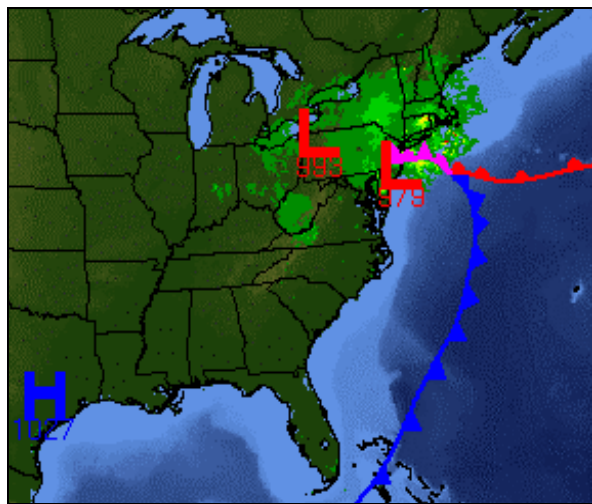


Figure 13. Same as Fig. 5, except for 1800 UTC 25 December 2002. The coastal low is near southern New Jersey and has a central pressure of 979 mb.

available to the storm. Such deep tropical moisture can be transported into the cold sector of a storm and cause large amounts of winter precipitation including snow, sleet, freezing rain and rain.

The Presidents' Day Snowstorm of 2003 produced frequent lightning along its cold front, as well as high snowfall totals in the Mid-Atlantic and southern New England states. However, the minimum central pressure never dropped below 1000 mb. Figure 15 shows CG flashes from the long-range lightning detection network within this extratropical cyclone between 0853 and 1153 UTC 16 February. Very frequent lightning was occurring within large areas of convection south of the storm center, along the cold front. The southerly flow associated with this system was transporting moisture northward into the Mid-Atlantic and Southern New England states where temperatures were well below freezing. Snowfall totals were generally between 2 and 4 feet (60 to 120 cm).

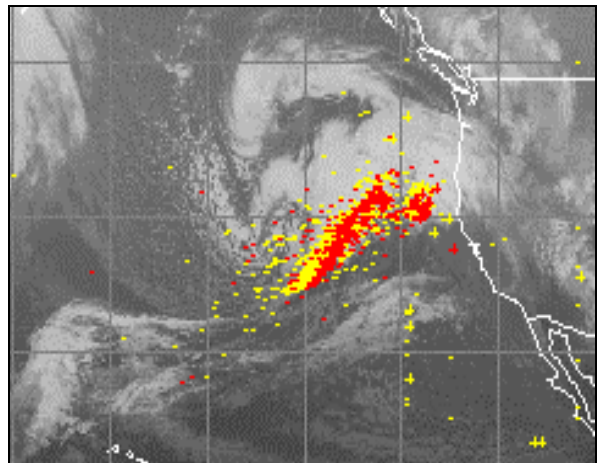


Figure 14. Same as Fig. 6, except for lightning between 1452 and 1752 UTC 18 December 2002. Satellite image is at 1752.

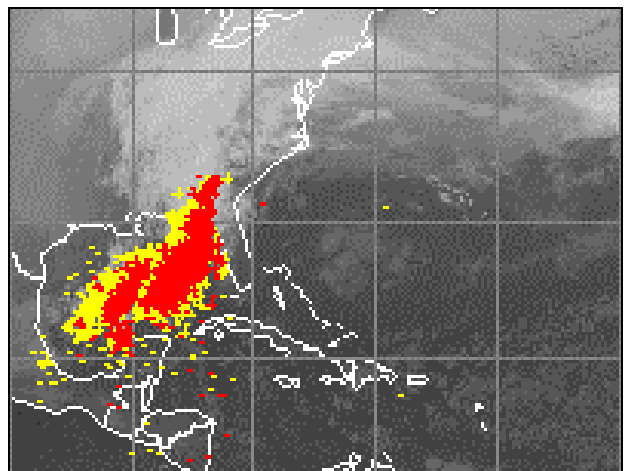


Figure 15. Same as Fig. 6, except for lightning from 0853 to 1153 UTC 16 February 2003. Satellite image is at 1153.

This example shows how the location and amount of lightning within extratropical cyclones can help determine its potential impacts. Extremely large amounts of lightning activity may be useful for precipitation nowcasting and forecasting.

4. TROPICAL CYCLONE LIGHTNING NOWCASTING APPLICATIONS

Section 4 will review how LLDN data over oceanic regions can be used to monitor tropical cyclones far from land. The LLDN continuously monitors lightning activity in tropical cyclones over a large portion of the Atlantic and Eastern Pacific tropical cyclone basins.

Lightning activity in tropical cyclones has been examined in several studies (Molinari et al., 1994; Molinari et al., 1999; Lyons and Keen, 1994; Black and Hallett, 1999; Cecil et al., 2002; Samsury and Orville, 1994). Most studies used NLDN data, and one used lightning detected by the Lightning Imaging Sensor (LIS) located onboard the Tropical Rainfall Measuring Mission (TRMM) satellite. Past analyses of lightning activity in tropical cyclones from the NLDN were limited to regions within ~400 km of the U.S. coastline. Analysis of lightning activity in tropical cyclones from LIS were limited to TRMM overpasses that occurred no more than twice a day for 90 seconds at a time.

Tropical depressions and tropical storms are generally more prolific lightning producers than hurricanes. Lightning activity in these systems does not show a preferential spatial pattern. New observations of CG lightning activity within numerous tropical cyclones over the Atlantic and Eastern Pacific Oceans away from land have reinforced many of the findings of Molinari et al. (1999). An extended description of these cases is in Demetriades and Holle (2005b).

Figure 16 shows the lightning activity produced by Tropical Storm Grace between 0952 and 1252 UTC 31 August 2003. Grace was located in the western Gulf of Mexico at this time and was a minimal tropical storm with sustained winds between 30 and 35 knots. This system was producing tremendous amounts of lightning shortly before it made landfall in southeast Texas.

Lightning does show preferential spatial patterns in hurricanes. The eyewall (or inner core) usually contains a weak maximum in lightning flash density. There is a well-defined minimum in flash density extending 80 to 100 km outside the eyewall maximum (Molinari et al., 1999). This is due to the stratiform rain processes that generally dominate most of the region of the central dense overcast. The outer rain bands typically contain a strong maximum in flash density. Figure 17 shows the lightning activity produced by Hurricane Isabel between 0354 and 0654 UTC 15 September 2003. Isabel was located just northeast of the Caribbean, in the western North Atlantic Ocean, and at this time was a borderline category 4 hurricane on the Saffir-Simpson Scale with sustained winds between 120 and 125 knots. Isabel was a powerful, organized hurricane at this time with a well-defined eye. The lightning activity in Isabel shows the typical pattern for well-organized hurricanes with a few flashes located in the eyewall and a high flash

density in the outer rain bands. The rain bands containing lightning were located on the southern and southeast sides of the hurricane at this time. Outer rain band lightning can be located anywhere within the periphery of a hurricane; it is not always located south and east of the center of circulation.

4.1 Outer Rainband Lightning

Lightning activity can help identify the most intense outer rainbands in a tropical cyclone. These rainbands often contain flooding rains and strong, gusty winds. Lightning can also show the evolution of growth and dissipation of outer rainbands as they rotate around the periphery of the storm. For many areas that do not experience the inner core of the hurricane, intense outer rainbands contain the most hazardous weather. Figure 18 shows CG lightning detected within Hurricane Ivan between 1345 and 1415 UTC 15 September 2004 as it

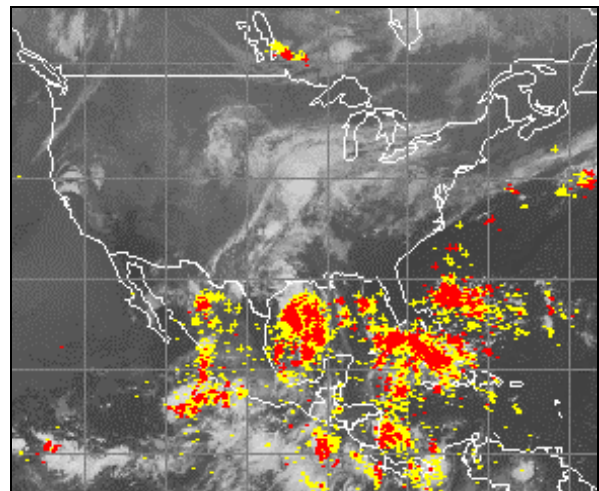


Figure 16. Same as Fig. 6, except for lightning detected in Tropical Storm Grace from 0952 to 1252 UTC 31 August 2003. Satellite image is at 1252 UTC.

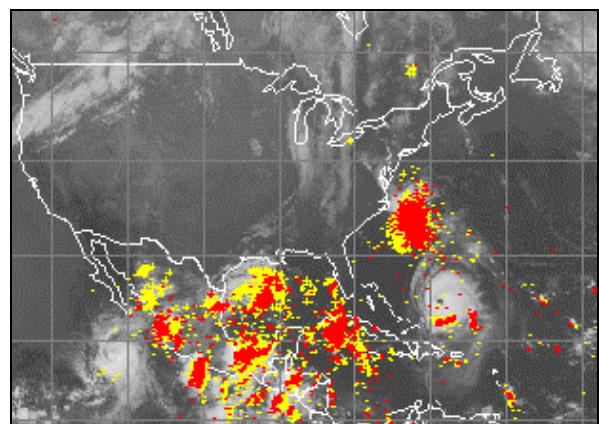


Figure 17. Same as Fig. 6, except for lightning detected in Hurricane Isabel from 0354 to 0654 UTC 15 September 2003. Satellite image is at 0654.

moved toward the U.S. coastline in the Gulf of Mexico. Lightning activity clearly delineates an intense outer rainband located on the east side of Ivan. Some other strong rainbands are shown by lightning data toward the south and southeast of the center of Ivan.

Hurricane Frances was a powerful category 3 hurricane on the Saffir-Simpson scale during the time period shown in Figure 19. Usually, high rates of lightning activity occur in one or two dominant rainbands located on one side of the hurricane. Frances was somewhat unique during this time as lightning activity indicated intense outer rainbands surrounding most of the periphery of the storm.

Figure 20 shows the evolution of an outer rainband as it rotates counterclockwise around the center of Hurricane Fabian on 5 September 2003. Between 1253 and 1553 UTC, lightning activity indicated that the most intense outer rainband rotated from a position located toward the east of the center of Fabian (yellow) to a position located to the north of Fabian (red).

In weaker tropical cyclones, such as tropical depressions and storms, intense rainbands often contain the highest wind speeds and heaviest rainfall. In order to properly issue tropical depression and storm advisories and warnings, it is critical to be able to identify the location and evolution of these features. Lightning activity provides a valuable dataset for

outer rainbands were identified by high rates of lightning activity located toward the southeast of Tropical Storm Kyle (Figure 21).

4.2 Eyewall Lightning

4.2.1 Methodology

For the eyewall study, tropical cyclones were examined only when they:

- Reached hurricane strength for at least 24 hours,
- Achieved category 3, 4 or 5 status on the Saffir-Simpson Scale at some point during their lifetime,
- Had their center within an area covered by at least 10% daytime CG lightning flash detection efficiency according to Vaisala's LLDN models.

The minimum CG lightning detection efficiency threshold of 10% means that the center of circulation for an Atlantic Basin hurricane had to be west of 65 W if the center was located south of 30 N, and west of 45 W if the center was north of 30 N. For Eastern Pacific Basin hurricanes, the center of the storm had to be located north of 20 N.

A 10% CG lightning detection threshold was chosen because it should still yield a relatively high detection efficiency for an eyewall lightning outbreak. Upon inspection of the Molinari et al. (1994, 1999)

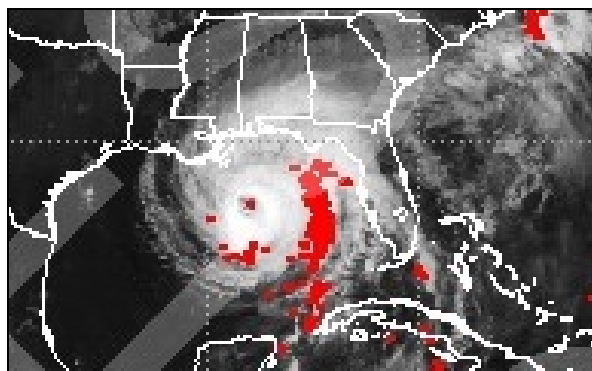


Figure 18. CG lightning detected in Hurricane Ivan between 1345 and 1415 UTC 15 September 2004.

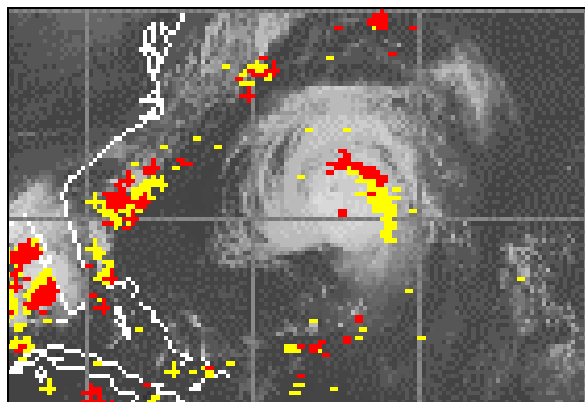


Figure 20. Same as Fig. 6, except for lightning detected in Hurricane Fabian from 1253 to 1553 UTC 5 September 2003.

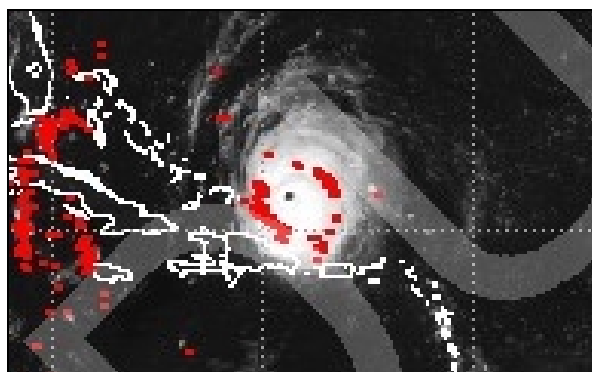


Figure 19. CG lightning detected in Hurricane Frances between 0945 and 1015 UTC 1 September 2004.

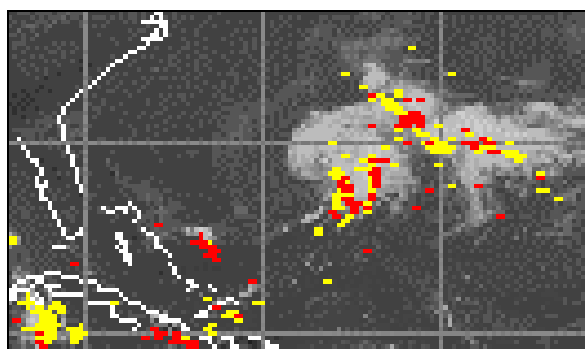


Figure 21. Same as Fig. 6, except for lightning detected in Tropical Storm Kyle from 1453 to 1753 UTC 2 October 2002.

hurricane lightning studies, the average eyewall CG lightning outbreak for Hurricanes Andrew, Elena, Hugo and Bob (1991) consisted of ~11 CG flashes. This is a conservative estimate because even within 400 km of the U.S. NLDN during the time periods in which these storms occurred, the CG lightning detection efficiency ranged between 20 and 80%. It is not an easy task to estimate the true number of CG lightning flashes per eyewall lightning outbreak. However, for the Molinari et al. (1994, 1999) studies we will assume that the average CG lightning flash detection efficiency for these four hurricanes was probably ~50%. Therefore, the average eyewall lightning outbreak for the hurricanes studied by Molinari et al. (1994, 1999) was ~22 flashes. Assuming a LLDN detection efficiency of 10% and an average eyewall lightning outbreak of 22 CG flashes, the eyewall lightning outbreak detection efficiency is ~90%. It should be noted that as these storms move closer to the coastline of the U.S. NLDN, the detection efficiency increases. Coastal areas of the U.S. have a CG lightning flash detection efficiency of 90%.

The position, maximum sustained wind speed and minimum central pressure of hurricanes used in this study were obtained from the best-track data produced by the National Hurricane Center (NHC) every 6 hours. Since a hurricane can propagate fairly long distances over a 6-hour period, the center position and minimum central pressure were interpolated between consecutive 6-hourly intervals in order to obtain 3-hour intervals for these variables.

In order to obtain eyewall lightning flash rates, Molinari et al. (1994, 1999) accumulated hourly CG lightning flash rates for all flashes that occurred within a 40 km radius around the center position of the hurricanes analyzed in their study. Weatherford and Gray (1988) found that the typical eyewall diameter (radius) of a hurricane is between 30 (15) and 60 (30) kilometers. For this study, 3-hourly CG lightning flash rates were obtained for all flashes occurring within 60 km of the center position of the hurricane. Each 3-hour interval was centered on the time of each center position estimated from the best-track data. For example, CG lightning would be accumulated within 60 km of the center position from 0130 to 0430 UTC for the 0300 UTC position estimate. Increasing the time interval and radius over which rates are accumulated should not have a significant impact on this study. Concentric eyewall cycles generally occur over time intervals of at least several hours and it is the presence of an eyewall lightning outbreak that is critical, not necessarily any instantaneous rate. Also, a 60 km radius should cause little contamination from lightning occurring in other parts of the hurricane because of the relative minimum in CG lightning that occurs in the inner rainbands (Molinari et al., 1999).

4.2.2 Eyewall lightning outbreaks

The LLDN has detected eyewall lightning outbreaks in many hurricanes from both the Atlantic and Eastern Pacific tropical cyclone basins during the past several years. The larger eyewall lightning outbreaks tend to occur on relatively small time and space scales.

Lightning bursts in the eyewalls of hurricanes sometimes rotate counterclockwise around the center of circulation for some distance before they dissipate. However, eyewall lightning outbreaks that were studied in several hurricanes since 2002 show that these outbreaks tend to preferentially occur on one side of the hurricane track. Several hours may separate consecutive bursts of eyewall lightning or these bursts may occur continually for 24-48 hours. Figure 22 shows lightning detected along the track of Hurricane Frances between 0000 UTC 3 September and 0000 UTC 4 September 2004. The track of Frances during this 24-hour period is shown by the white line. Three eyewall lightning outbreaks can be identified as Frances moved toward the northwest. All three of the outbreaks occurred on the northeast side of the storm track. The first outbreak is shown in green, the second outbreak in orange and the final outbreak on this day in red.

Eyewall lightning tends to occur when the inner core of the hurricane is undergoing a change in structure and intensity. Lightning helps to identify intense convective cores with larger updraft speeds embedded in the eyewalls of hurricanes. These lightning outbreaks may be strongly, and perhaps uniquely, associated with tall precipitation features, often called hot towers, that form in hurricane eyewalls. In favorable environments for hurricane intensification, these tall precipitation features are often associated with rapid intensification of hurricanes. Vaisala continues to collaborate with the tropical meteorology community in order to determine how often eyewall lightning outbreaks are associated with tall precipitation features within hurricane eyewalls. If a strong association is found, LLDN data may provide a valuable data set for the tropical cyclone nowcasting community.

4.2.3 Concentric eyewall cycles

Outbreaks of lightning within the eyewalls of moderate-to-strong hurricanes were studied by Molinari et al. (1999), who proposed that outbreaks of eyewall lightning were generally caused by either eyewall contraction or secondary eyewall replacement. Therefore, eyewall lightning outbreaks may be able to help forecasters nowcast hurricane intensification (eyewall contraction) or weakening (secondary eyewall replacement). The study by Molinari et al. (1999) was limited to 5 Atlantic basin hurricanes where the center of circulation passed within 400 km of one of the NLDN sensors. Sugita and Matsui (2004) performed a similar analysis on two typhoons that were within range of the Japanese Lightning Detection Network operated by Franklin Japan Corporation. Lightning does not always occur in the eyewall of a hurricane. However, when lightning does occur it may be a sign of change within the hurricane inner-core structure that could help nowcast storm intensity.

The relationship between eyewall lightning outbreaks and concentric eyewall cycles has been studied for numerous hurricanes and typhoons in the Atlantic, Eastern Pacific, and western Pacific since 2002. Twenty-three of the 25 secondary eyewall formations or secondary eyewall contractions studied

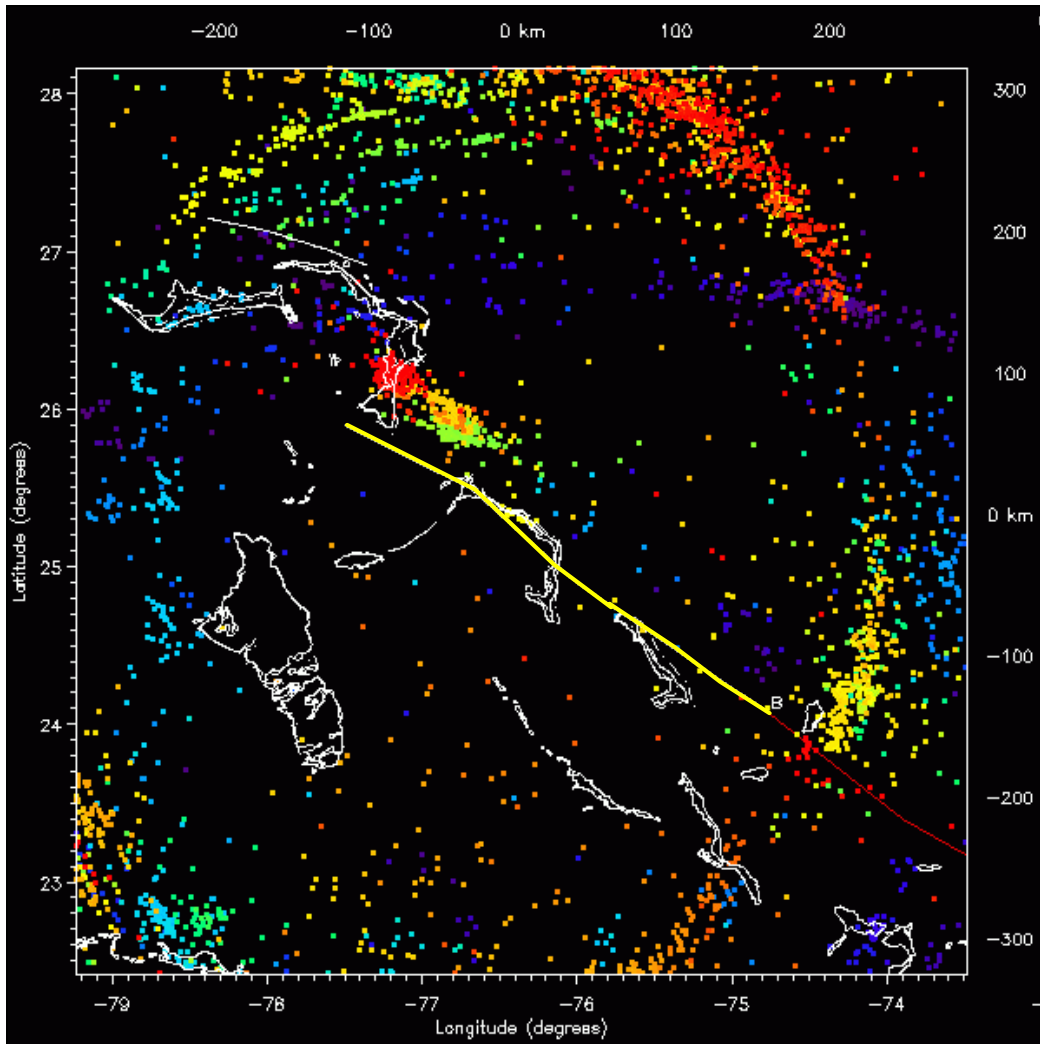


Figure 22. CG lightning detected by the LLDN in Hurricane Frances between 0000 UTC 3 September and 0000 UTC 4 September 2004. The track of the center of Frances during this 24-hour period is shown by the yellow line. Three bursts of eyewall lightning are along the right side of the track of Frances as the storm moved toward the northwest (upper left). The first burst of eyewall lightning is in green, the second burst is in orange, and the third burst is in red.

were associated with eyewall lightning outbreaks. The locations of these discreet lightning bursts may aid forecasters when trying to identify secondary eyewall formation and secondary eyewall contraction. The former situations implies that the rapid intensification of a hurricane is coming to an end, and the latter situation implies that the hurricane is about ready to rapidly intensify.

4.2.4 Hurricane Charley

Charley developed just east of the Windward Islands and moved WNW into the Caribbean Sea. Charley then turned to the north and made landfall as a category 1 hurricane in western Cuba on 13 August. After crossing Cuba, Charley rapidly intensified and turned NNE, making landfall near Charlotte Harbor, Florida at ~2030 UTC 13 August. Charley attained

category 4 status shortly before landfall and reached a maximum intensity of 125 knots.

Eyewall lightning from Hurricane Charley was analyzed for the 19 hours preceding landfall. Data were not analyzed before this time period due to high center position error estimates by the NHC, and poor LLDN geometry relative to Charley's position on 11-12 August. Figure 23 shows the eyewall flash rate superimposed on central pressure. Low-to-moderate rates of eyewall lightning occurred as Charley intensified at a moderate rate between 0300 and 1200 UTC. As the primary eyewall of Charley contracted and the storm rapidly intensified, eyewall flash rates increased dramatically. LLDN eyewall flash rates increased to 230 and 340 at 1500 and 1800 UTC, respectively. At this time, a secondary eyewall developed around the primary eyewall. The high flash rates at 2100 UTC may be at least partially due to landfall of Charley at ~2030 UTC.

4.2.5 Hurricane Lili

Lili developed southeast of the Lesser Antilles islands and moved through the Caribbean to western mainland Cuba before continuing through the Gulf of Mexico, eventually making landfall in Louisiana on 3 October. Lili intensified to category 4 status on the Saffir-Simpson Scale on 2 October and reached a maximum intensity of 125 knots.

Figure 24 shows the eyewall lightning flash rate superimposed upon observations of central pressure. On 30 September a short outbreak of lightning occurred near the center of the storm as the eyewall started to form and Lili achieved hurricane status. A second outbreak occurred early on 1 October as the eyewall started to show some decay. This decay was most likely caused by interaction with land in western Cuba. Another outbreak occurred near 2100 UTC 1 October. This lightning activity occurred during a secondary eyewall formation and replacement cycle. The NHC discussion from 0300 UTC 2 October stated "Lili appears to have just completed an eyewall replacement cycle based on the last 2 recon passes through the center." The secondary eyewall contraction caused rapid intensification as pressures fell from ~970 to ~955 mb in 12 hours.

Shortly after this time period another eyewall lightning outbreak occurred during the time that a secondary eyewall formation was speculated by NHC. The NHC discussion from 0900 UTC 2 October stated "Aerial reconnaissance data showed a fairly rapid central pressure fall...to about 954 mb just before 0600 Z...but a later dropsonde from a NOAA aircraft of 955 mb suggested that the central pressure had leveled...this is probably temporary...and some short-term fluctuations in strength are likely due to internal processes such as eyewall replacement cycles."

A final outbreak of eyewall lightning occurred between 1500 UTC 2 October and 0600 UTC 3 October. This outbreak contained the largest eyewall lightning rates recorded in this study and in Molinari et al. (1994, 1999). Flash rates peaked at over 600 per 3-hour interval. This outbreak was not only associated with the development of an outer eyewall, but it was also associated with an unexplained rapid weakening that dropped Hurricane Lili from a category 4 storm to a category 2 storm within 12 hours. The NHC discussion from 2100 UTC 2 October stated "Lili is showing signs of peaking...as the aircraft and satellite imagery indicate the beginning of an outer eyewall that will likely bring a halt to the current intensification."

4.3 Lack of Eyewall Lightning

The present study has found evidence to support the Molinari et al. (1999) hypothesis that a hurricane that has been fairly steady in intensity will remain fairly steady in intensity when little or no eyewall lightning is present. Therefore, a lack of eyewall lightning or very low eyewall lightning rates may be another valuable tool that can aid forecasters in hurricane nowcasting.

Hurricane Isabel had a long period without eyewall lightning while it was very strong. The storm developed

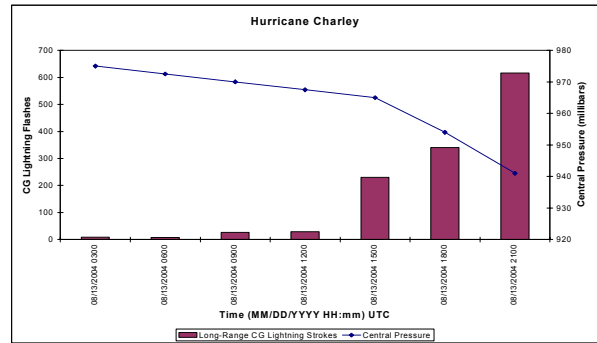


Figure 23. Three-hour CG lightning rates detected within 60 km of Hurricane Charley's center superimposed on Charley's central pressure. Lightning rates are purple bars with values located on left y-axis, and central pressure is the blue line with values on right y-axis.

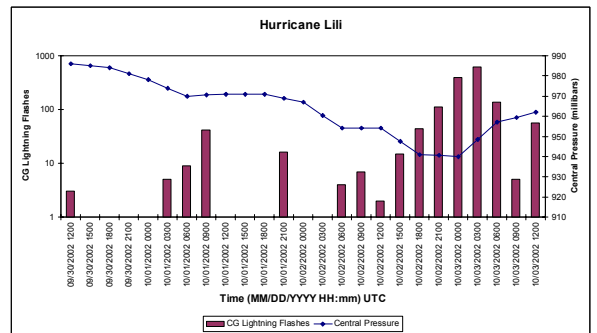


Figure 24. Same as Figure 23, except for Hurricane Lili.

west of Africa and moved WNW to the NE of the Caribbean islands. Isabel made landfall on the North Carolina coast on 18 September as a category 2 hurricane with sustained winds of 90 knots. On 11 September Isabel intensified to category 5 status on the Saffir-Simpson Scale and reached a maximum intensity of 145 knots. Isabel had already reached its maximum intensity before reaching the 10% CG lightning detection efficiency contour off the coast of the U.S. Figure 25 shows the eyewall flash rate superimposed upon observations of central pressure from Hurricane Isabel during the period of analysis. One eyewall lightning flash was detected near 1200 UTC 14 September as the storm was about to undergo a fairly rapid weakening stage. Another eyewall lightning outbreak occurred between 0900 UTC 15 September and 0300 UTC 16 September. There was only a total of 5 CG flashes detected, however they occurred during a time period of concentric eyewall formation. The NHC discussion at 0900 UTC 15 September stated "The aircraft has also reported well-defined concentric wind maxima." Isabel maintained a fairly steady central pressure between 1200 UTC 16 September and 0900 UTC 18 September. During this time period, no eyewall lightning was detected in this storm. This is in agreement with the Molinari et al. (1999) hypothesis that hurricanes undergoing little change in intensity will not exhibit eyewall flashes. A final outbreak of eyewall lightning

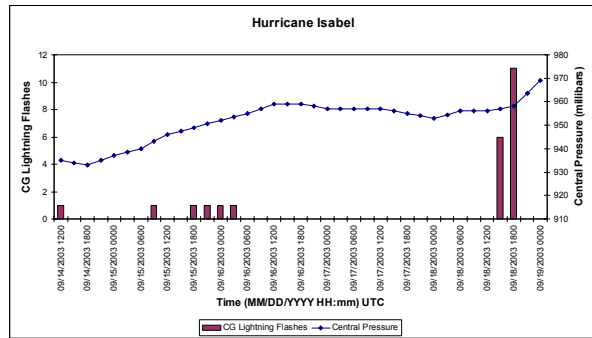


Figure 25. Same as Figure 23, except for Hurricane Isabel.

occurred between 1500 and 1800 UTC 18 September. This outbreak was probably initially caused by concentric eyewall formation before being influenced by landfall. The NHC discussion at 0900 UTC 18 September stated “WSR-88D radar data from Morehead City shows what looks like a classic concentric eyewall formation...with a poorly-defined ring of convection near the center and a stronger ring 40-50 nm out.”

5. CONCLUSIONS

Lightning data over otherwise data-sparse regions are expected to be valuable for meteorologists. Flash information is especially important for nowcasting and forecasting for aviation and maritime interests. In addition, long-range CG flash data identifies convection that can have significant subsequent impacts on land areas adjacent to oceans. Both extratropical and tropical regions can benefit from data from the LLDN.

In extratropical cyclones, a variety of situations have been described where lightning data over the oceans have the potential to be very useful sources of information about convection. The existence of CG flashes at specific times and locations over the ocean helps identify features that form and intensify extratropical cyclones. The spatial and temporal extent, and the pattern of such flashes can also be useful for diagnosing the stage and extent of development of such systems. Flash data can be assimilated continuously into numerical weather prediction models to better identify the presence of latent heat release that strongly influences the progression of the track and intensity of cyclonic systems in the model (Pessi et al., 2004). In addition the time, location, and amount of upstream lightning may identify deep moisture that can be important in producing heavy downstream precipitation, including frozen precipitation on the ground in winter. The vertical structure of cold pools also may be identified with flash data.

In tropical cyclones, LLDN data may provide forecasters a valuable diagnostic tool for observing concentric eyewall cycles and other important dynamic changes in the core of a hurricane, since concentric eyewall cycles are often obscured on visible and infrared satellite imagery. Observations from this study suggest that eyewall lightning outbreaks occur when there is a change in the dynamic structure of the eyewall

or center of circulation. Outbreaks were often observed when the eyewall became ragged or elongated in shape, dry air started to intrude on the storm center, a hurricane came under the influence of increased vertical wind shear, or during landfall. In addition, lightning in the outer rainbands may identify which bands are the most intense. For areas outside the inner core, and in weaker tropical cyclones, intense rainbands often contain the highest wind speeds and heaviest rainfall. Appropriate advisories and warnings need to be able to identify the location and evolution of such outer rainbands in those situations.

REFERENCES

- Alexander, G.D., J.A. Weinman, V.M. Karyampudi, W.S. Olson, and A.C. Lee, 1999: The impact of the assimilation of rain rates from satellites and lightning on forecasts of the 1993 Superstorm. *Mon. Wea. Rev.*, **127**, 1433-1457.
- Atallah, E.H., and L.R. Bosart, 2003: The extratropical transition and precipitation distribution of Hurricane Floyd (1999). *Mon. Wea. Rev.*, **131**, 1063-1081.
- Black, R.A., and J. Hallett, 1999: Electrification of the hurricane. *J. Atmos. Sci.*, **56**, 2004-2028.
- Cecil, D.J., E.J. Zipser and S.W. Nesbitt., 2002: Reflectivity, ice scattering, and lightning characteristics of hurricane eyewalls and rainbands. Part I: Quantitative description. *Mon. Wea. Rev.*, **130**, 769-784.
- Chang, D.-E., J.A. Weinman, C.A. Morales, and W.S. Olson, 2001: The effect of spaceborne microwave and ground-based continuous lightning measurements on forecasts of the 1998 Groundhog-Day storm. *Mon. Wea. Rev.*, **129**, 1809-1833.
- Demetriades, N.W.S., and R.L. Holle, 2005a: Lightning produced by cold season oceanic extratropical cyclones: Observations related to nowcasting storm development, intensity and precipitation amounts. *Preprints, Conf. on Meteor. Appl. of Lightning Data*, San Diego, Jan. 9-13, Amer. Meteor. Soc., 7 pp.
- , and —, 2005b: Long-range lightning applications for hurricane intensity and precipitation nowcasting. *Preprints, Conf. on Meteor. Appl. of Lightning Data*, San Diego, Jan. 9-13, Amer. Meteor. Soc., 9 pp.
- Lyons, W.A., and C.S. Keen, 1994: Observations of lightning in convective supercells within tropical storms and hurricanes. *Mon. Wea. Rev.*, **122**, 1897-1916.
- Martin, J.E. and J.A. Otkin, 2004: The rapid growth and decay of an extratropical cyclone over the Central Pacific Ocean. *Wea. Forecast.*, **19**, 358-376.
- Molinari, J., P. Moore, and V. Idone, 1999: Convective structure of hurricanes as revealed by lightning locations. *Mon. Wea. Rev.*, **127**, 520-534.
- , P.K. Moore, V.P. Idone, R.W. Henderson, and A.B. Saljoughy, 1994: Cloud-to-ground lightning in Hurricane Andrew. *J. Geophys. Res.*, **99**, 16665-16676.

- Nierow, A., R.C. Showalter, F.R. Mosher, and T. Lindholm, 2002: Mitigating the impact of oceanic weather hazards on transoceanic flights. *Preprints, 17th Intl. Lightning Detection Conf.*, Tucson, Arizona, October 16-18, Vaisala, 4 pp.
- Pessi, A., S. Businger, K.L. Cummins, and T. Turner, 2004: On the relationship between lightning and convective rainfall over the central Pacific Ocean. *Preprints, 18th Intl. Lightning Detection Conf.*, June 7-9, Helsinki, Finland, Vaisala, 9 pp.
- Reed, R.J. and M.D. Albright, 1986: A case study of explosive cyclogenesis in the Eastern Pacific. *Mon. Wea. Rev.*, **114**, 2297-2319.
- Samsury, C.E., and R.E. Orville, 1994: Cloud-to-ground lightning in tropical cyclones: A study of Hurricanes Hugo (1989) and Jerry (1989). *Mon. Wea. Rev.*, **122**, 1887-1896.
- Sugita, A., and M. Matsui, 2004: Lightning in typhoons observed by JLDN. *Proceedings, 18th Intl. Lightning Detection Conf.*, June 7-9, Helsinki, Finland, Vaisala, 4 pp.
- Weatherford, C. and W.M. Gray, 1988: Typhoon structure as revealed by aircraft reconnaissance. Part II: Structural variability. *Mon. Wea. Rev.*, **116**, 1044-1056.